International Journal of Earth Sciences Knowledge and Applications
www.ijeska.com

Research Article e-ISSN: 2687-5993

# Resistivity Contrast and the Phenomenon of Geophysical Anomaly in Groundwater Exploration in A Crystalline Basement Environment, Southwestern Nigeria

**Bawallah Musa Adesola[1], Adiat Kola Abdul-Nafiu[1], Akinlalu Ayokunle Adewale[1], Ilugbo Stephen Olubusola*[1], Akinluyi Francis Omowonuola[2], Ojo Bosede Taiwo[1], Oyedele Akintunde Akinola[3], Bamisaye Oluseyi Adunola[4], Olutomilola Olabode Olusola[5], Magawata Usman Zayyanu[6]**

[1]*Department of Applied Geophysics, Federal University of Technology, Akure, Nigeria*
[2]*Department of Remote Sensing and GIS, Federal University of Technology Akure, Ondo State, Nigeria*
[3]*Department of Physics, Ekiti State University, Ado-Ekiti, Nigeria*
[4]*Department of Applied Geology, Federal University of Technology, Akure, Nigeria*
[5]*Department of Geology, Afe Babalola University, Ado Ekiti, Nigeria*
[6]*Department of Physics Kebbi State University of Science and Technology, Aliero, Kebbi State, Nigeria*

**INFORMATION**

**Article history**
Received 15 September 2020
Revised 26 October 2020
Accepted 30 October 2020
Available 15 December 2020

**Keywords**
Lateral Resistivity Profiling
Vertical Electrical Sounding
M-formula
Groundwater Yield
Akure Metropolis

**Contact**
*Ilugbo Stephen Olubusola
E-mail: bussytex4peace44@gmail.com
https://orcid.org/0000-0002-1001-4815

**ABSTRACT**

In absence of magnetic, gravity, electromagnetic and seismic refraction tools, Lateral Resistivity Profiling (LRP) has been engaged as major tool in the study of deep-seated geological structures for the evaluation of structural trend and settings for groundwater exploration in a complex geologic environment of Southwestern Nigeria. Twenty LRP using wenner configuration was used to delineate zones of resistivity contrast anomaly (weak zone) diagnostic of fracture, fault, cracks, joints and highly weathered geologic materials. Thirty-three Vertical Electrical Sounding (VES) using schlumberger configurations was carried out on the zones of resistivity contrast (weak zones) to delineate geoelectric sequence and layer stratification. The results from the VES were used to generate geoelectric section, geoelectric maps and also to determine the second order parameters. Groundwater potential map was also generated from the integration of geoelectric parameters using Multi-Criteria Evaluation Techniques (MCDA). The model was classified into low, moderate, high and very high groundwater potential zones and all identified points was drilled and the boreholes was very productive, which were used to validate the accuracy of the groundwater potential map. M-formula was used to determine the groundwater yield index value to model the groundwater yield map. All the result obtained has been found to be very relevant in groundwater evaluation of the study area and thereby justifying the relevance of LRP as a major tool in groundwater exploration before carrying out VES.

## 1. Introduction

The challenges facing scientist especially geoscientists in developing countries such as Nigeria is very daunting in the face of lack of adequate facilities and equipment for research and development. Therefore, where there is lack of tools and the scientist must make an impact in an ever-increasing challenging world, the capacity for survival becomes inevitable. The scientists and researcher are faced with a herculean task of proving his worth in order to be of service to immediate society and to make necessary contributions for the development of environment and humanity in general (Oyedele et al., 2020). Obviously, the need for creativity, innovations and ingenuity comes into play, where a researcher must make an impact for the development of society in this chosen field of study. Where there is clear wide gap in terms of provisions for equipment, materials and research facilities. This research effort was carried out as a way to fill this wide gap, especially in an attempt to make water available for domestic, agriculture as well as industrial usage through exploration and exploitation of water resources in a typical crystalline basement complex environment of southwestern Nigeria (Oyedele, 2019; Ozegin et al., 2019; Ilugbo et al., 2019; Bawallah et al., 2020). Public water utilities and dam for irrigation are fast becoming things of the past to be able to strike good success in the search for water (Alabi et al., 2019). It is important to engage complimentary exploration tools such as ground magnetic, electromagnetic, seismic refraction and electrical resistivity methods to be able to properly define structural setting, depositional nature, structural trends and layer stratification for a proper evaluation of basement rock for groundwater exploration and exploitation (Olorunfemi et al., 1991; Ilugbo and Adebiyi, 2017; Ilugbo et al., 2018a; Bawallah et al., 2018; Adebo et al., 2018; Adebo et al., 2019). But most times, the research is seriously handicap by lack of facilities, where only one equipment is available to carryout investigation instead of using different equipment's; such was the situation of this research work.

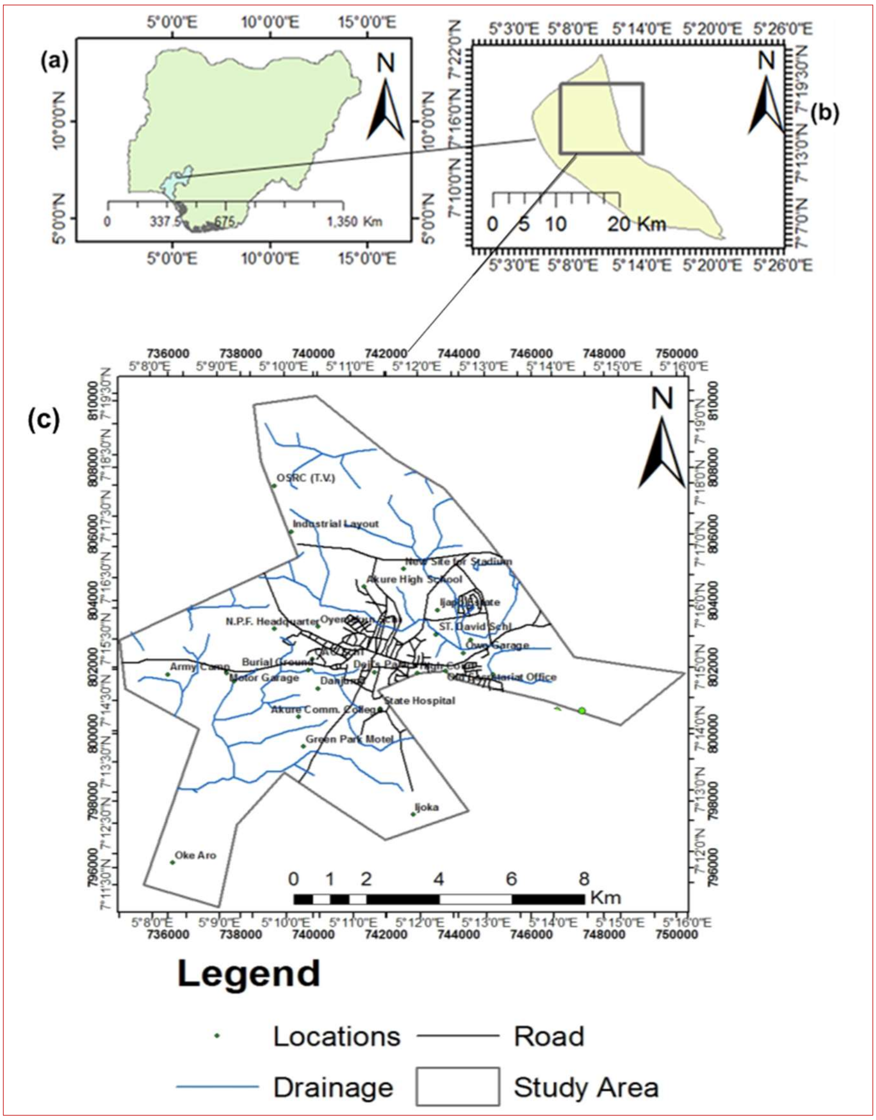


Fig. 1. (a) Map of Nigeria and Ondo State showing Akure Metropolis, (b) Map of Akure Metropolis showing the location area (c) Location map showing the study area

However, very worrisome that often rather than run a compressive survey using innovation and creativity, most researchers rather result to random sampling approach using only VES technique. This is rather unscientific and it is taking us to nowhere in crystalline environment with complex geology. Therefore, there is the very need to fill this gap through LRP tools using wenner profiling or dipole-dipole to delineate geology structures that maybe favourable to groundwater accumulation and sustainability before embarking on the VES technique as a follow up. Therefore, this approach has been adopted in this study for a compressive groundwater evaluation, exploration and exploitation within Akure metropolis, Southwestern basement complex region of Nigeria.

## 2. Site Description and Geology of the Study Area

The study area falls within Akure metropolis, Ondo State, Southwestern Nigeria. It lies between latitude 798000N to 810000N and longitude 734700E to 746200E (Fig. 1). It is well accessible through several road networks within and around the study area. The study area can be described as moderately undulating and the drainage pattern is dendritic. The study area is underlain by rocks of the Precambrian Basement Complex of Southwestern Nigeria (Rahaman, 1989).

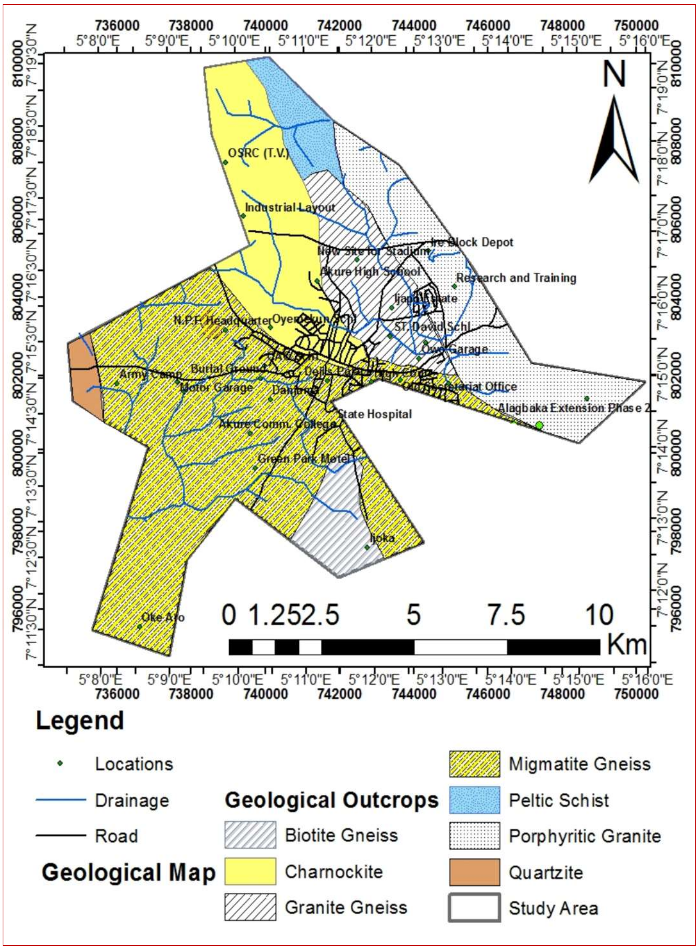


Fig. 2. Geological map of the study area

The geological mapping and other related studies of the area around the Akure Metropolis have been carried out by several workers amongst who are (Owoyemi, 1996; Olarewaju, 1988; Odeyemi et al., 1999; Aluko, 2008; Slomczynska, 2004; Adebiyi et al., 2018). The area around the Akure Metropolis is underlain by eight petrological units of the Basement Complex of Southwestern Nigeria identified by (Rahaman, 1988) and also described by (Olarewaju, 1988; Rahaman, 1988; Aluko, 2008). These are migmatitegneiss, quartzite, charnockitic, biotite gneiss, migmatite gneiss, pelti schist, granite gneiss and porphyritic granite (Fig. 2).

## 3. Methodology

Two techniques were adopted for this research work; the LRP techniques using wenner configuration was engaged as a tool in place of susceptibility or conductivity or density contrast for the reconnaissance survey to delineate structural settings/trends and depositions, while the VES technique was engaged using schlumberger configuration for geoelectric sequence/layer stratification (Fig. 3).

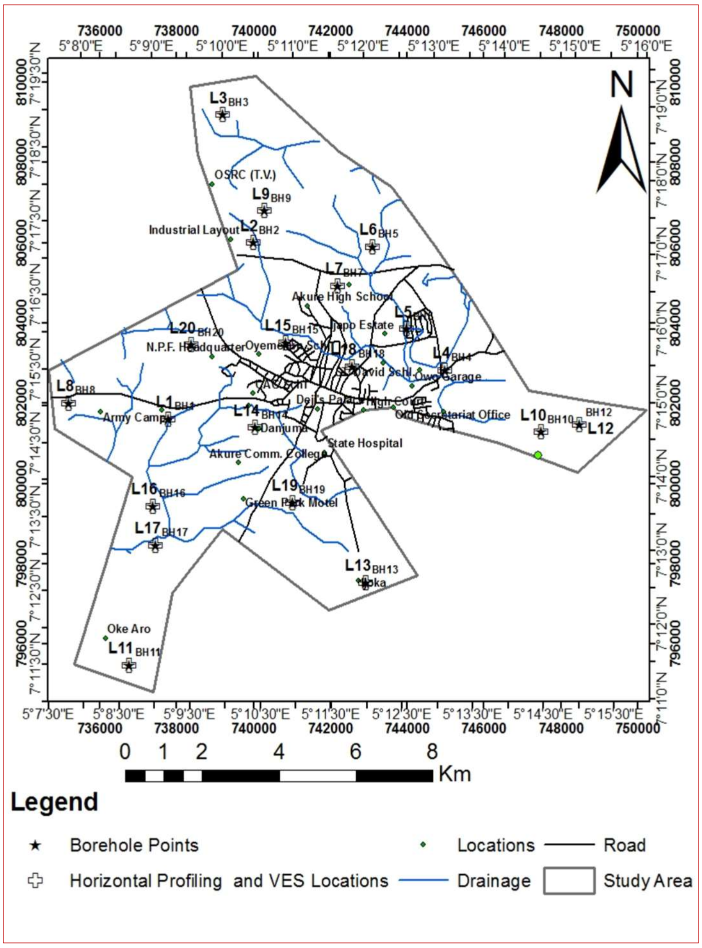


Fig. 3. Data acquisitions map of the study area

The LRP was carried out in twenty (20) locations within the study area and thirty-three (33) VES points were selected on the basics of zones of resistivity contrasts (weak zones). The weak zone delineated from the LRP result was used to model anomalous zone map while the results obtained from VES were used to determine the second order parameters (Dar-Zarrouk). The Dar-Zarrouk parameters obtained from the first order parameters (geoelectric parameters) which are Total longitudinal unit conductance (S), Total transverse unit resistance (T), and coefficient of anisotropy (λ) using below mathematical expressions.

$$S = \sum_{i=1}^{N} \frac{h_i}{\rho_i} \quad (\Omega^{-1} \text{or Siemens}) \tag{1}$$

and

$$T = \sum_{i=1}^{N} \rho_i h_i \quad (\Omega m^2) \tag{2}$$

When a number of layers with thicknesses of $h_1$, $h_2$, $h_3$, transverse resistances of $T_1$, $T_2$, $T_3$, ….., and conductance of $S_1$, $S_2$, $S_3$, respectively, are involved in a geoelectrical section, their total longitudinal conductance (S) or total transverse resistance (T) may have to be considered (Murali and Patangay, 1998) and are given by:

$$S = S_1 + S_2 + S_3 + \ldots\ldots\ldots \quad \text{where } S_1 = \frac{h_1}{\rho_1} \tag{3}$$

and

$$T = T_1 + T_2 + T_3 + \ldots\ldots\ldots \quad \text{where } T_1 = h_1 \rho_1 \tag{4}$$

If the total thickness of the layers in the geoelectrical section considered is H, then the average longitudinal resistivity $\rho_l$ is given by:

$$\rho_l = \sum i = 1 \frac{hi}{Si} \tag{5}$$

and the average transverse resistance $\rho_t$ is given by:

$$\rho_t = \sum i = 1 \frac{Ti}{hi} \tag{6}$$

where $\rho_t$ is always greater than $\rho_l$. Therefore, the entire section will thus be always anisotropic (Singhal and Niwas (1981). with regard to electrical resistivity. The coefficient of electrical anisotropy is defined as:

$$\lambda = \sqrt{\frac{\rho t}{\rho l}} \tag{7}$$

Integration geophysical parameters were used to develop a groundwater potential model for the area. In this present study, the choice among a set of zones for evaluation of groundwater prospect has been based upon multiple criteria such as coefficient of anisotropy, overburden thickness, aquifer resistivity, aquifer thickness and geological. The process is known as MCDA using analytic hierarchy process (AHP).

For a Multi-criterial Modelling, firstly a template has been created by identifying the quadtrees used in the analysis. The number of inputs quadtrees that can be selected is reduced to one less than the total number. A default weight is calculated by dividing 100 by the number of quadtrees used in the overlay and is assigned to each quadtree class (Chowdhury et al., 2009; Ewusi et al., 2009; Lee et al., 2012; Adiat et al., 2013; Ilugbo et al., 2018a). Each class is labeled with the short legend title taken from the input quadtree. Different categories of derived thematic maps have been assigned scores in a numerical scale of 1 to 5 depending upon their suitability to holding capacity of groundwater (Eastman, 1996; Navalgund, 1997). A summation of these values led to the generation of final weight map. Mathematically, this can be defined as:

$$GW = f(CA, OT, AR, AT, G) \tag{8}$$

where, GW is groundwater, CA is coefficient of anisotropy, OT is overburden thickness, AR is aquifer resistivity, AT is the aquifer thickness and G is geological map. The weighted linear combination (WLC) is applied according to the following equation to estimate the Groundwater Prospect Index (GWPI). This technique is usually specified in terms of normalized weightings (w) for each criterion as well as rating scores (R) for all classes relative to each of the criteria. The final utility GWPI for each option $O_i$ is then calculated as follows:

$$GWPI = W_i R_i \tag{9}$$

where, GWPI is the groundwater potential index value $W_i$ is the weight (w) of parameter i and $R_i$ is the rating score (R) of parameter *i*. Therefore, the groundwater prospect index (GWPI) for each location was computed using

$$GWPI = CA_W CA_R + OT_W OT_R + AR_w AR_R + AT_w AT_R + G_W G_R \quad 10)$$

The subscripts w and R indicate weights and ratings for each parameter. Also, the groundwater yield, Y of the study area was determined using M-formula (Bawallah et al., 2018; Ilugbo et al., 2018b). The relationship is shown as:

$$Y = \lambda \, x \, T \tag{11}$$

## 4. Results and Discussion

### 4.1. LRP

All the horizontal profiling was taken along E – W directions, Location 1 (Fig. 4a) cover a distance of 75 m. Three (3) major weak zones (anomalous zone) constituting region of resistivity contrast were identified which is a diagnostic of fracture, fault, joints, crack or zones of highly weathered geologic materials at distance of 15 m, 45 m and 75 m.

These points are the regions considered for further investigation in other to define the nature and extent of anomaly using VES. The same approach was carried out in Location 2 (Fig. 4b) but contrary to the situation obtained in Location 1, the apparent resistivity was generally low. The profile three was characterized by generally low apparent resistivity with variation between 30 Ωm to 130 Ωm (Fig. 4c).

The profile was indicative of the presence of highly weathered crystalline basement rock that has probably weathered into clay and for the purpose of comparison; two zones were considered for further investigation. These were region of moderately high and low anomalous zone at a distance of 30 m and 50 m with resistivity of 60 Ωm and 40 Ωm.

Location 4 (Fig. 4d) was characterized with resistivity variation ranging from 240 to 400 Ωm and there was no observable major or minor anomalous zone indicated along this profile. However, the region of lowest resistivity at distance of 2 m was considered.

Location 5 (Fig. 4e) cover a distance of 50 m with three anomalous zone of resistivity contrast which occurred at 10 m, 20 m and 30 m. the major anomalous zone was observed at 10 m. The region of lowest apparent resistivity anomalous zone was observed at 30 m in Location 6 (Fig. 4f) with resistivity of 800 Ωm. Two zones/region were considered at Location 7 (Fig. 4g) at a distance of 20 m and 30 m.

Location 8 (Fig. 4h) was characterized with two major zones of resistivity contrast which occurred at a distance of 30 m, 35 m. Two major resistivity contrast (anomalous zones) were observed at Location 9 (Fig. 4i) at a distance of 10 m and 40 m. The entire location is generally not suitable for groundwater prospecting but two observable major zones of anomaly were identified.

Location 10 (Fig. 4j) was characterized by apparently low resistivity with one major zone of resistivity contrast occurring at 15 m. The major zone of resistivity anomaly (weak zone) was obtained at 20 m at Location 11 (Fig. 4k). Location 12 (Fig. 4l) exhibited generally low resistivity throughout the entire profile with resistivity variation ranging between 42 to 50 Ωm, reflecting that the area was predominantly clayey in nature which is indicative of low groundwater prospect. Therefore, the highest point of resistivity contrast of 50 Ωm was considered. Two anomalous zones were identified at a distance of 30 m and 55 m within Location 13 (Fig. 4m).

Location 14 (Fig. 4n) was characterized by resistivity variation between 120 to 180 Ωm, with a downward trend obtained from the midpoint of the profile which indicate increase in weathering and fracturing activities towards the western end of the area. This implies that prospecting for water will be most probably better from the mid-point and toward the western plank with two major resistivity contrasts was identified at 20 m and 35 m.

The profile exhibited moderately high resistivity with resistivity variation ranging between 250 to 350 Ωm at Location 15 (Fig. 4o). Two major zones of interest/region of anomaly were observed at 5 m and 30 m while the entire profile has highly resistive geologic materials with resistivity variation between 320 to 420 Ωm at Location 16 (Fig. 4p) with weak zone indicated at 25 m.

Location 17 (Fig. 4q) showed one major and minor anomalous zone diagnostic of fracture/highly weathered geologic materials with resistivity variation of 160 Ωm and 235 Ωm while the major and minor zones of resistivity anomaly were identified. The profile displayed moderately high apparent resistivity while resistivity distribution reduces gradually towards the western part of the study location (Fig. 4r) and the weak zone was observed at a distance of 35 along the profile.

Fig. 4s shows high resistivity which is indicative of the presence of near surface horizon crystalline basement rock and the anomaly point of interest was obtained at a distance of 25 m along the profile. Four major points of anomalous zones were observed at Location 20 at a distance of 2 m, 20 m, 40 m and 50 m (Fig. 4t). The anomalous zone at 2 m was considered to be the better prospect for groundwater with resistivity of 120 Ωm. The entire anomalous zone (weak zones) across the entire location areas were subjected to further investigation using VES.

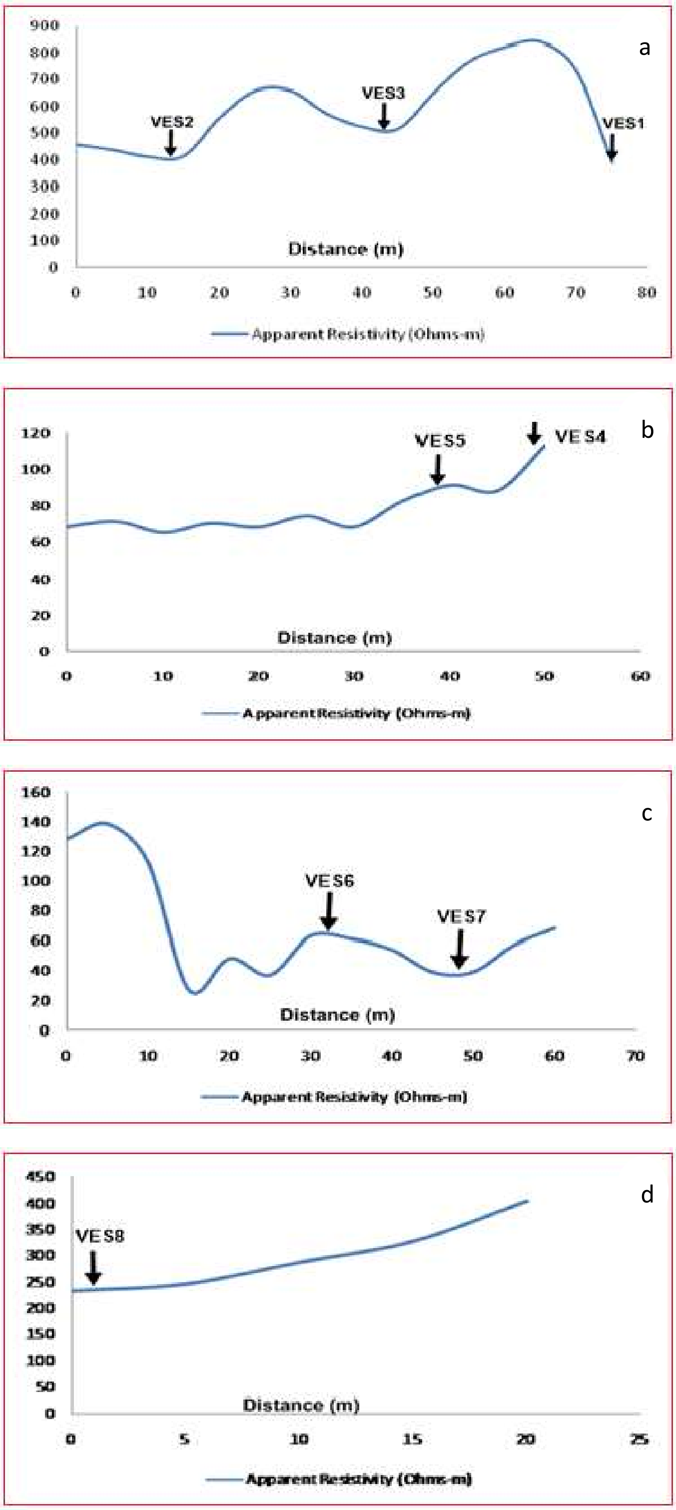

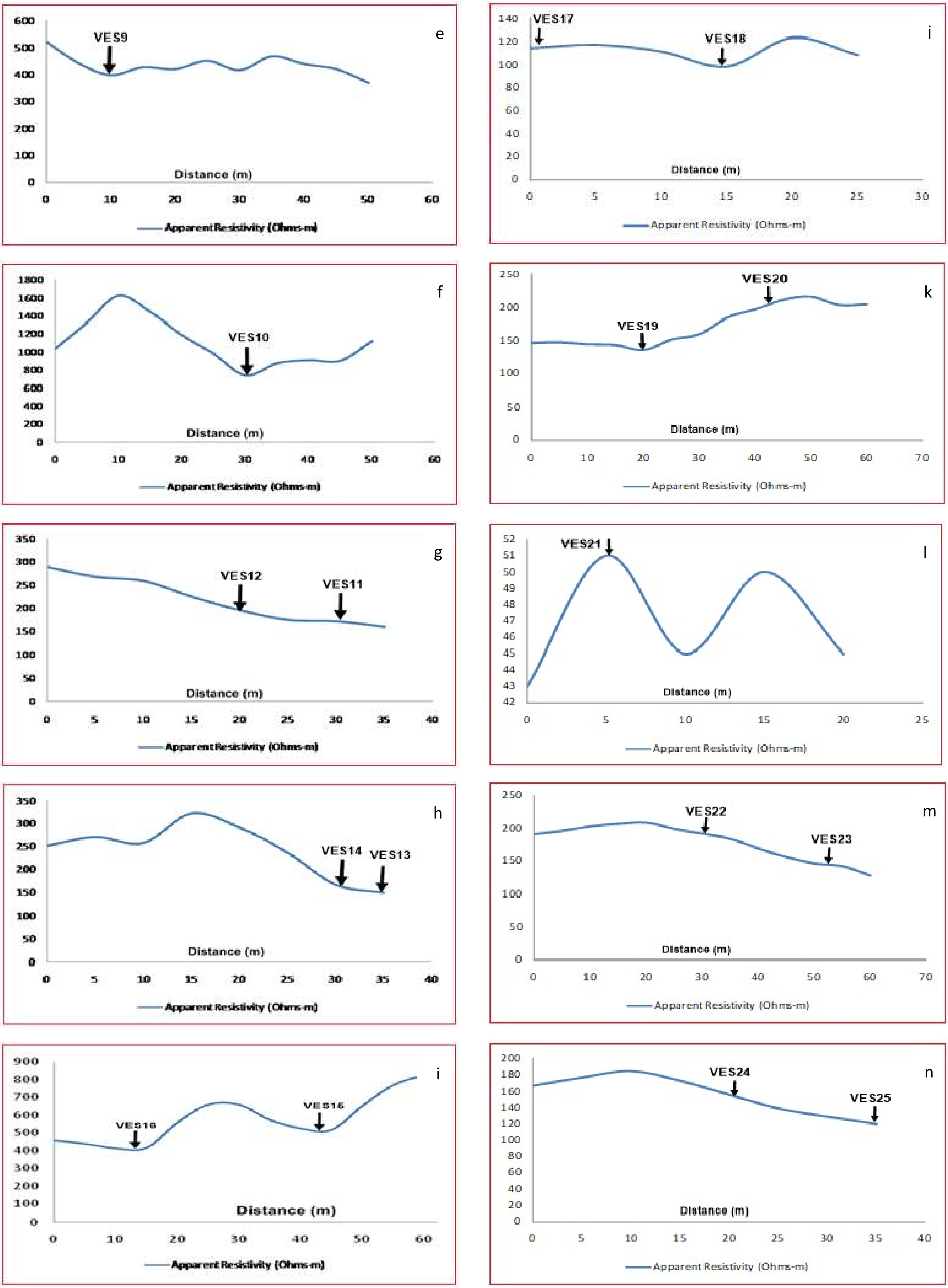
e
VES9
Distance (m)
Apparent Resistivity (Ohms-m)
j
VES17
VES18
Distance (m)
Apparent Resistivity (Ohms-m)
f
VES10
Distance (m)
Apparent Resistivity (Ohms-m)
k
VES19
VES20
Distance (m)
Apparent Resistivity (Ohms-m)
g
VES12
VES11
Distance (m)
Apparent Resistivity (Ohms-m)
l
VES21
Distance (m)
Apparent Resistivity (Ohms-m)
h
VES14
VES13
Distance (m)
Apparent Resistivity (Ohms-m)
m
VES22
VES23
Distance (m)
Apparent Resistivity (Ohms-m)
i
VES16
VES15
Distance (m)
Apparent Resistivity (Ohms-m)
n
VES24
VES25
Distance (m)
Apparent Resistivity (Ohms-m)

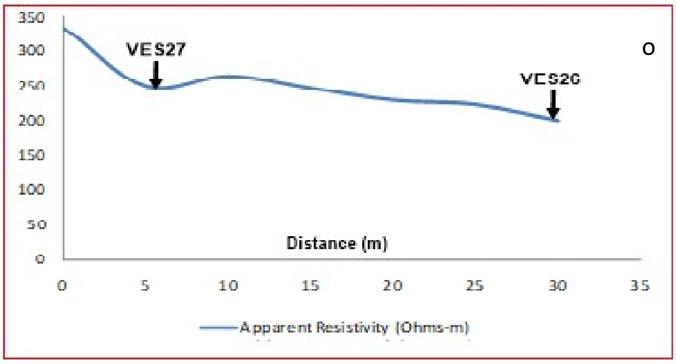


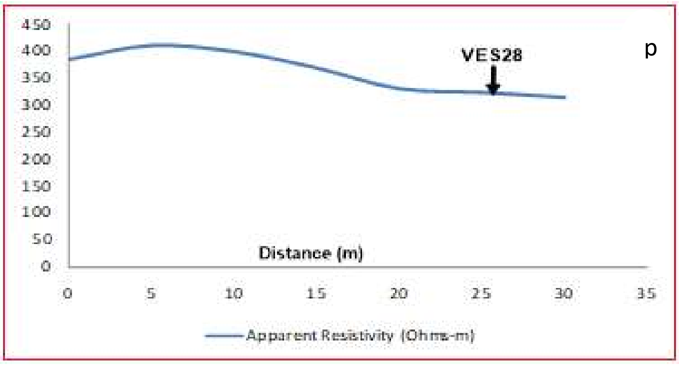


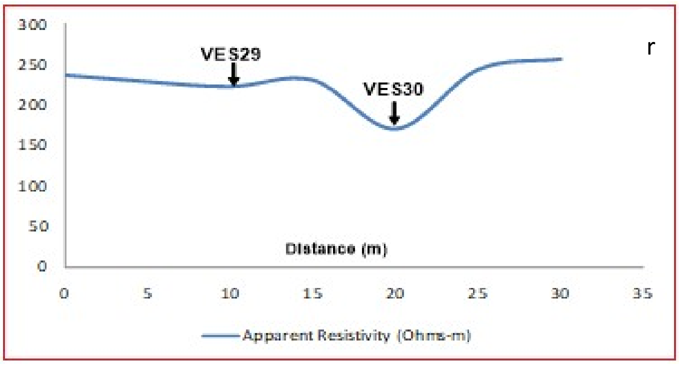


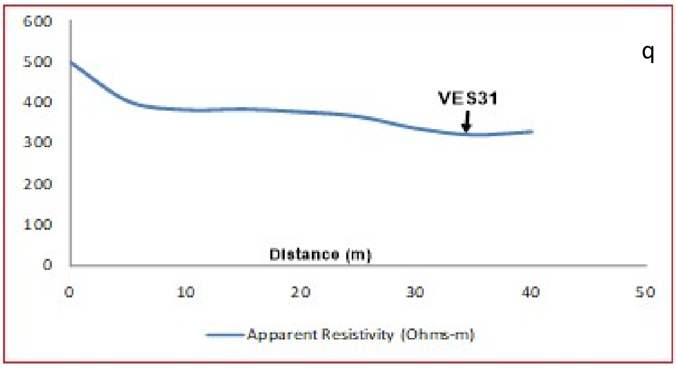


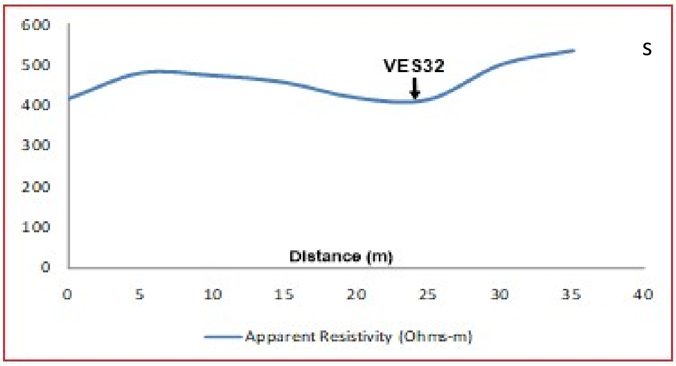


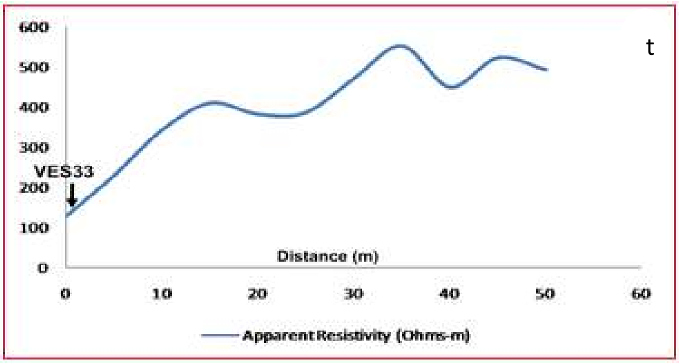


Fig. 4. Horizontal profiling's on; (a) Location 1, (b) Location 2, (c) Location 3, (d) Location 4, (e) Location 5, (f) Location 6, (g) Location 7, (h) Location 8, (i) Location 9, (j) Location 10, (k) Location 11, (l) Location 12, (m) Location 13, (n) Location 14, (o) Location 15, (p) Location 16, (r) Location 17, (q) Location 18, (s) Location 19 and (t) Location 20

### 4.2. Anomalous zone/Resistivity contrast map

The anomalous zones represent regions of resistivity contrasts resulting from zones of weakness arising from fault, fracture, crack, joints and highly weathered materials. The map was developed by contouring the resistivity anomaly/contrasts measurement obtained on each point of the twenty LRP carried out within the study area (Fig. 5).

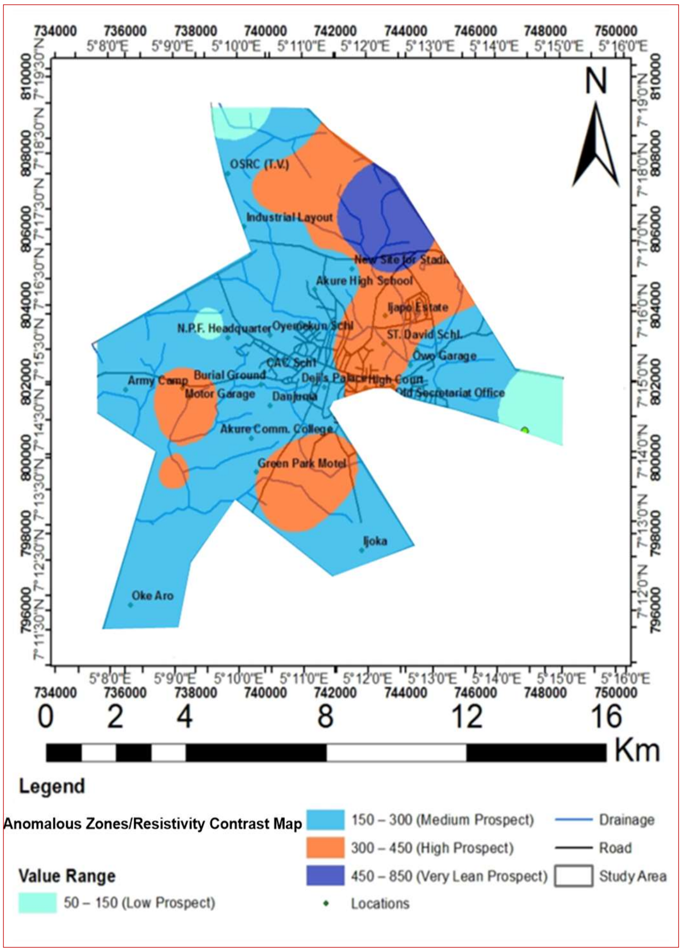


Fig. 5. Anomalous Zone/Resistivity Contrast map of the study area

The map shows reasonable information on the hydro-geological settings of the area as well as structural settings at 20 m depth with AB/3 of 60 m. four distinct hydrological settings were identified and classified into zones of water bearing/hydrological formations which are low, medium, high and lean water prospect with resistivity distribution ranging from 50 to 100 Ωm, 100 to 300 Ωm, 300 to 4500 Ωm and 450 to 850 Ωm.

The extreme north, central and the entire southwestern part was categorized as medium water bearing formation/ prospect, while more than sixty percent of the northeastern and eastern parts has a high-water bearing formation/ prospect. Furthermore, small portion at the northeastern part is considered as very lean water bearing prospect and fringe at the northwestern and southeastern end is categorized as low water bearing formation/prospect.

### 4.3. VES

#### 4.3.1. Characteristic of the VES curves

Curves types identified ranges from A, H, HA, KH, HK and HKH varying between three to five geoelectric layers and HA curve type was predominating (Fig. 6). Typical curve types in the area are as shown in Fig.7(a-f).

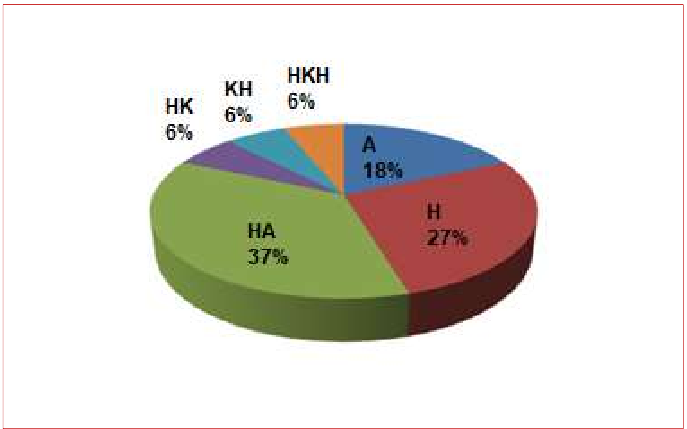


Fig. 6. Typical curves of the study area

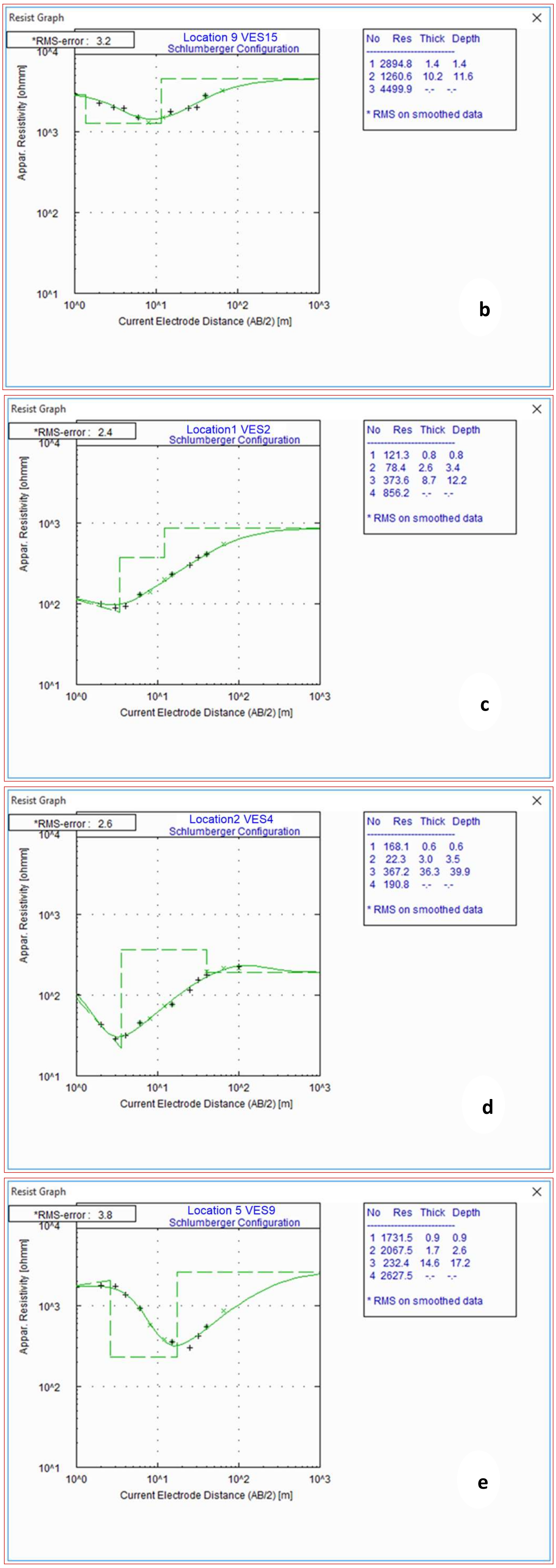


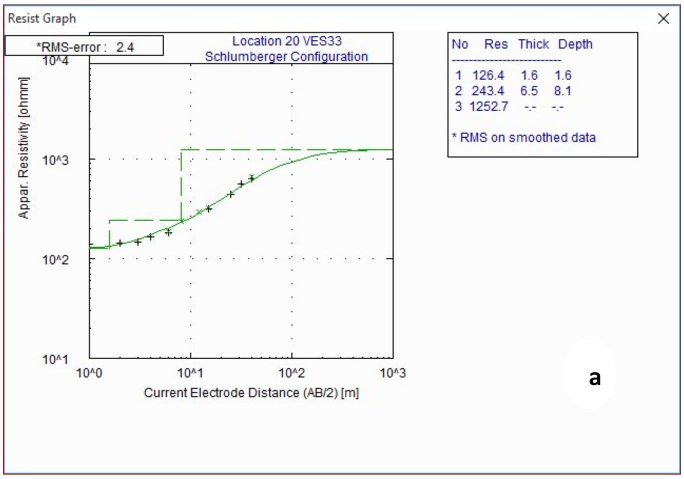

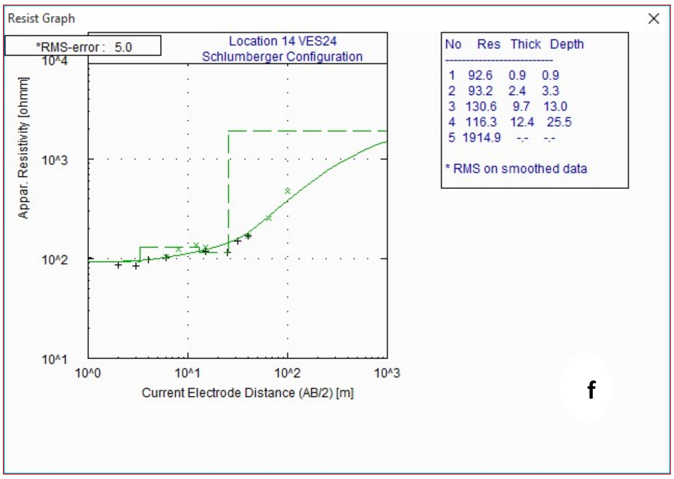


Fig. 7. Typical curve type of the study area; a: A type, b: H type, c: HA type, d: HK type, e: KH type and f: HKH type

### 4.3.2. Geoelectric and Lithological Characteristic within the Study Location

The geoelectric sections were represented by the 2-D view of the geoelectric parameters (depth and resistivity) derived from the inversion of the electrical resistivity sounding data. The geoelectric section cut through SW–NE and NW–SE directions within the study location (Fig. 8).

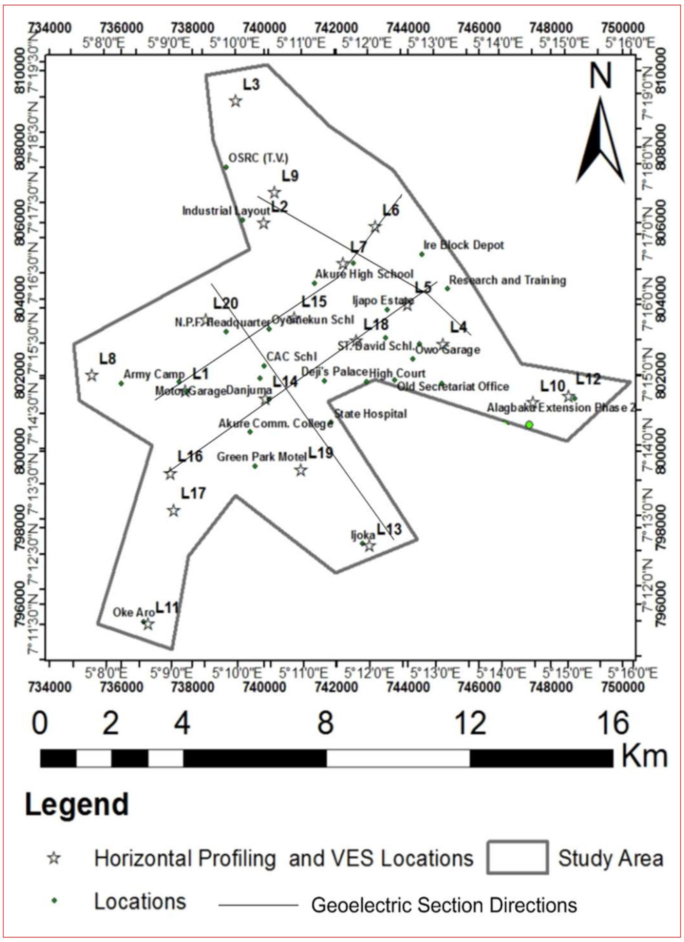


Fig. 8. Geoelectric section direction within the study area

The geoelectric sections along SW–NE and NW–SE directions identified three to five geoelectric/geologic subsurface layers within the area (Figs. 9a to 9d). From the geoelectric section, the topsoil, weathered layer, weathered/ fractured basement and fresh basement were determined.

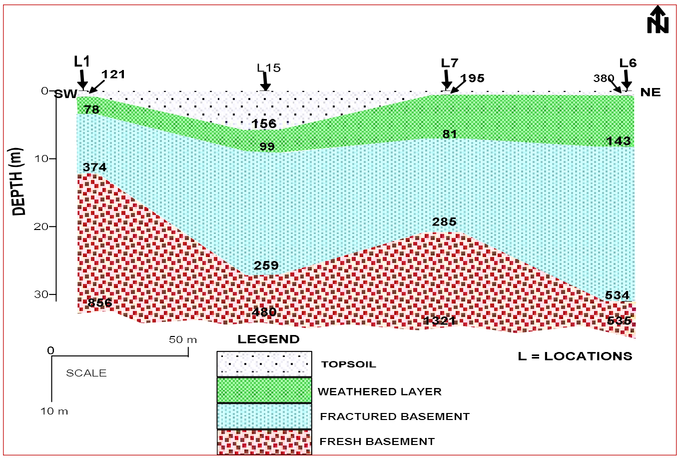


Fig. 9a. Geoelectric section along SW–NE direction

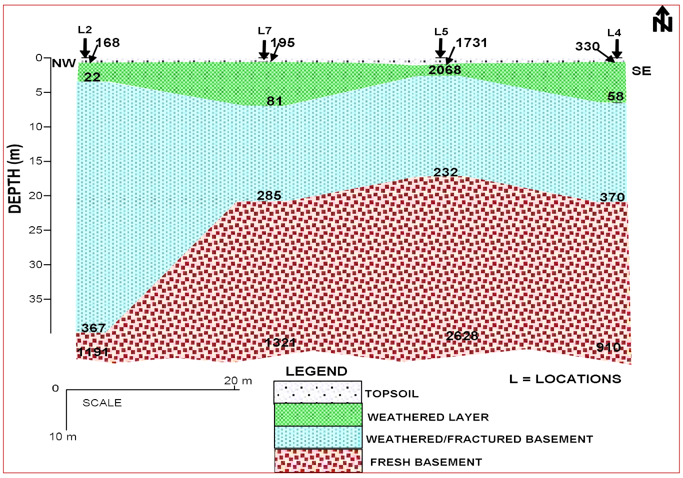


Fig. 9b. Geoelectric section along NW–SE direction

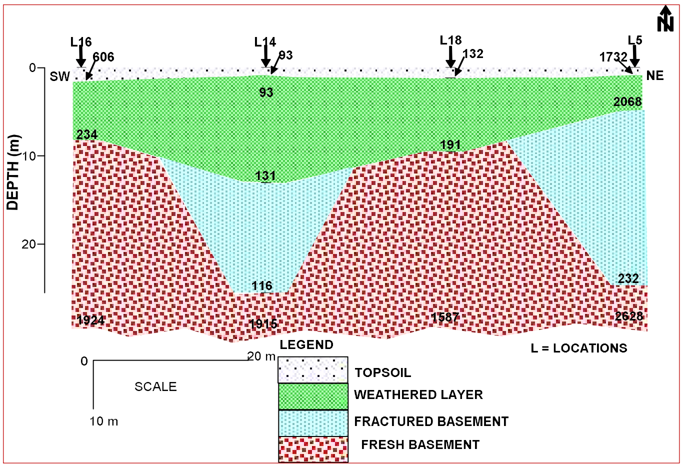


Fig. 9c. Geoelectric section along SW–NE direction

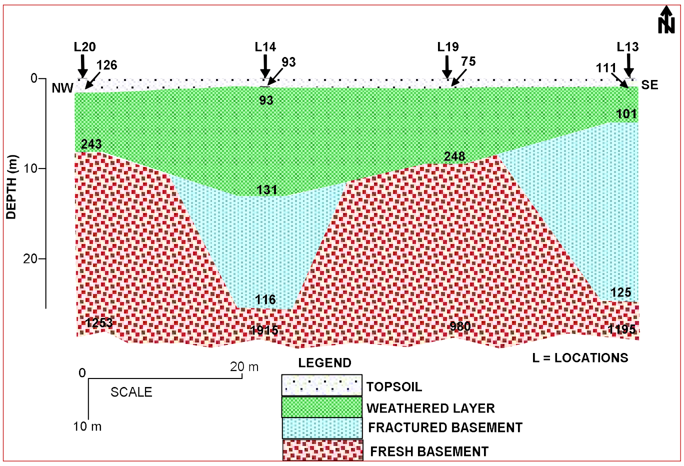


Fig. 9d. Geoelectric section along NW–SE direction

The topsoil comprising of clay, clayey sand and sandy clay with the resistivity values ranging from 75 to 1732 Ωm with its thickness varying from 0.5 to 1.6 m. The weathered layer comprising of clay, clayey sand and sandy clay with resistivity varying 22 to 2068 Ωm and thickness ranges from 3.3 to 13 m.

The weathered/fractured basement has a resistivity value ranging from 116 to 370 Ωm with its thickness varying from 12.2 to 39.9 m while the fresh base-ment has a resistivity value ranging from 535 to 2626 Ωm with depth to basement ranging from 6.7 to 39.9 m. Weathered and fracture basement constitute the aquifer unit within the investigated location.

### 4.4. Geoelectric maps

#### 4.4.1. Aquifer resistivity map

Fig. 10 shows aquifer resistivity map with four distinctive aqueferous zone. Area characterized by low resistivity aquifer zone located at the fringe of the eastern, western and southwestern part. Region of moderate aquifer resistivity with value ranging from 100 to 150 Ωm was indicated at fringe of southern, southwestern and a small closure at the northern part.

High aquifer resistivity dominates 80% of the entire study area with resistivity varies from 150 to 250 Ωm while moderately low was observed as a small closure point within the area. It was inferring that the greater part of the study area has the propensity for high groundwater prospect while these resistivity factor can be considered as indicative of higher pore spaces that will allow for greater porosity and permeability of the water bearing formation within the investigated area.

#### 4.4.2. Aquifer thickness map

The map was generated with a view to account for the various aquifer thicknesses that obtained with the view that aquifer thickness remains an important factor in groundwater productivity and evaluation, since it holds one of the major keys to groundwater accumulation and storage. Therefore, this map was categorized into four aquifer thickness zones vis-à-vis very low, low, moderate and high (Fig. 11).

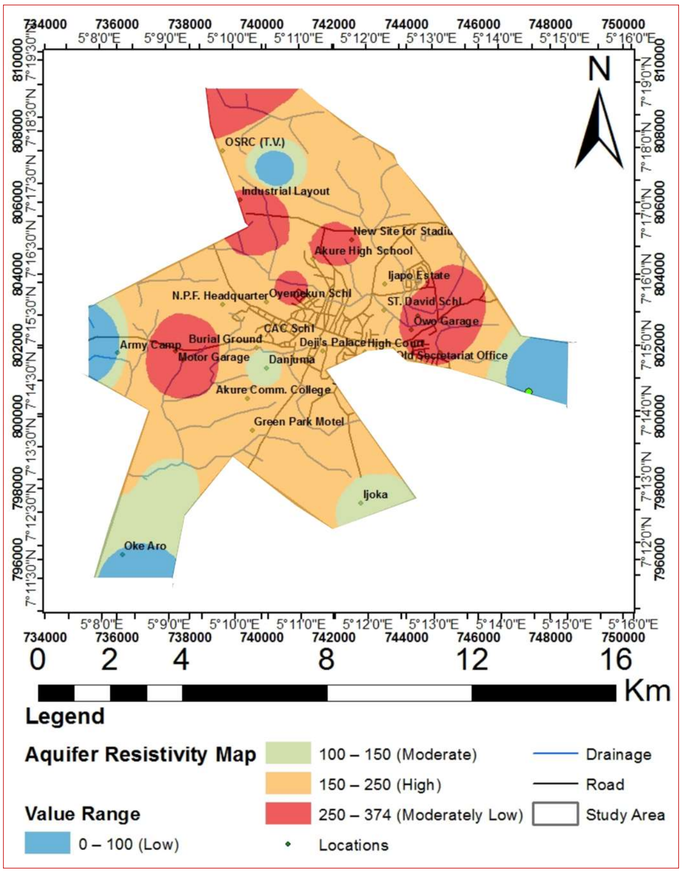


Fig. 10. Aquifer resistivity map of the study area

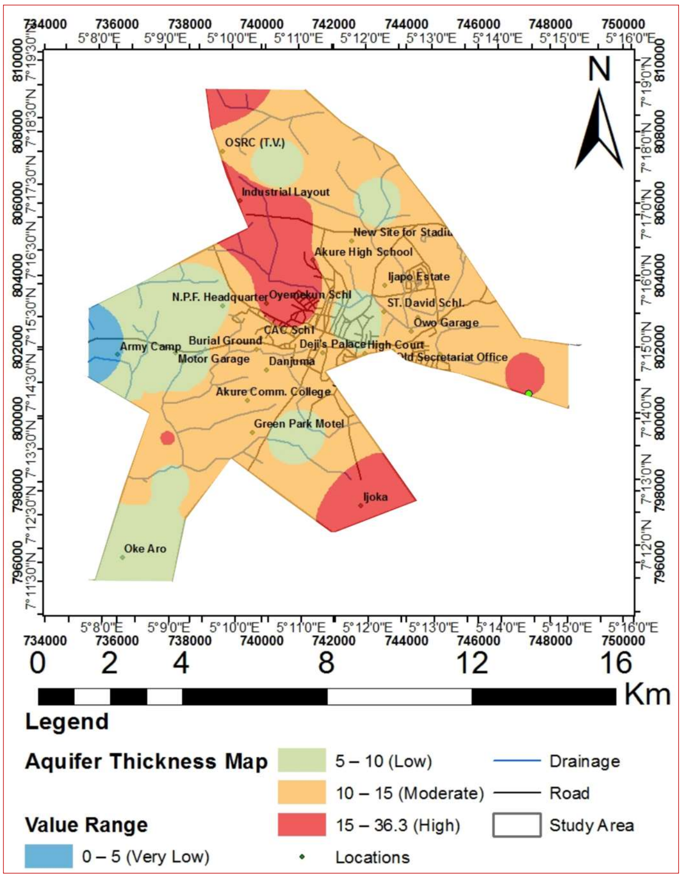


Fig. 11. Aquifer thickness map of the study area

### 4.4.3. Overburden thickness map

The overburden thickness in this study is assumed to include the topsoil, the weathered layer and fractured basement. Hence the established depths to bedrock beneath all the VES stations were used to produce the overburden thickness map (Fig. 12). The overburden thickness varies from 6.7 m to 39.9 m. The map shows areas of high overburden thickness in the northwestern, north eastern, central and a small closure at the southeastern parts which favors the ground-water resources in the area particularly when underlain by weathered/ fractured basement and fractured bedrock. These areas correspond to basement depressions which are groundwater convergent zones. Hence, they are relatively good prospect for groundwater development.

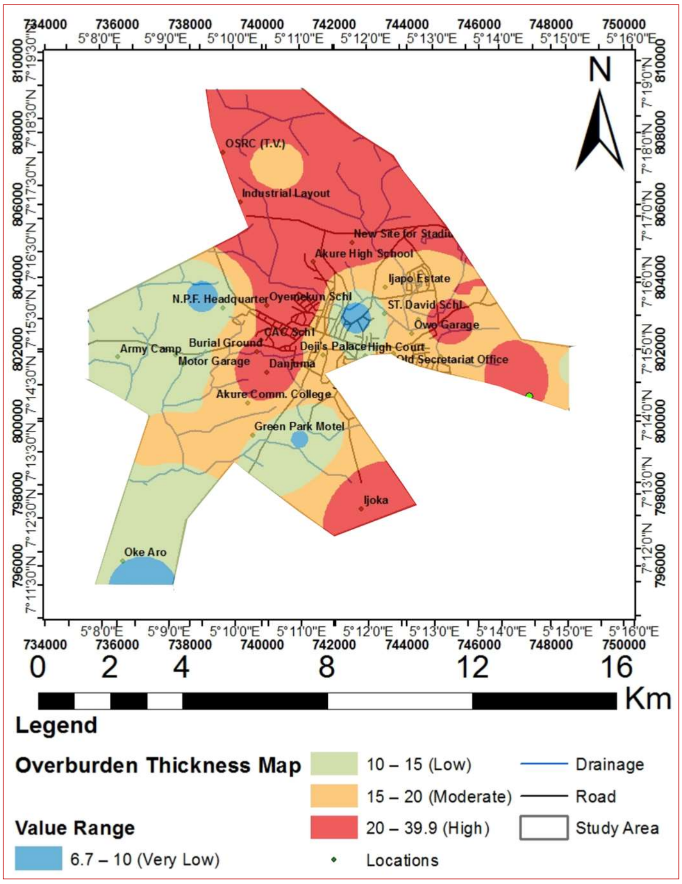


Fig. 12. Overburden thickness map of the study area

### 4.5. Dar Zarrouk Parameters for Groundwater Characteristics

The coefficient of anisotropy is estimated along with the secondary geoelectric parameters. The estimation shows that the longitudinal conductance varies from 0.008 to 0.43 $\Omega^{-1}$ in the area (Fig. 13). The qualitative use of this parameter is to demarcate changes in total thickness of low resistivity materials. The transverse resistance ranges from 1000 to 17000 Ωm which gives information both about the thickness and resistivity of the area (Fig. 14). Based on these estimates it was found that the coefficient of anisotropy ranges from 1.o to 1.9, which depicts the true variation of the anisotropy character of rock formation (Fig. 15).

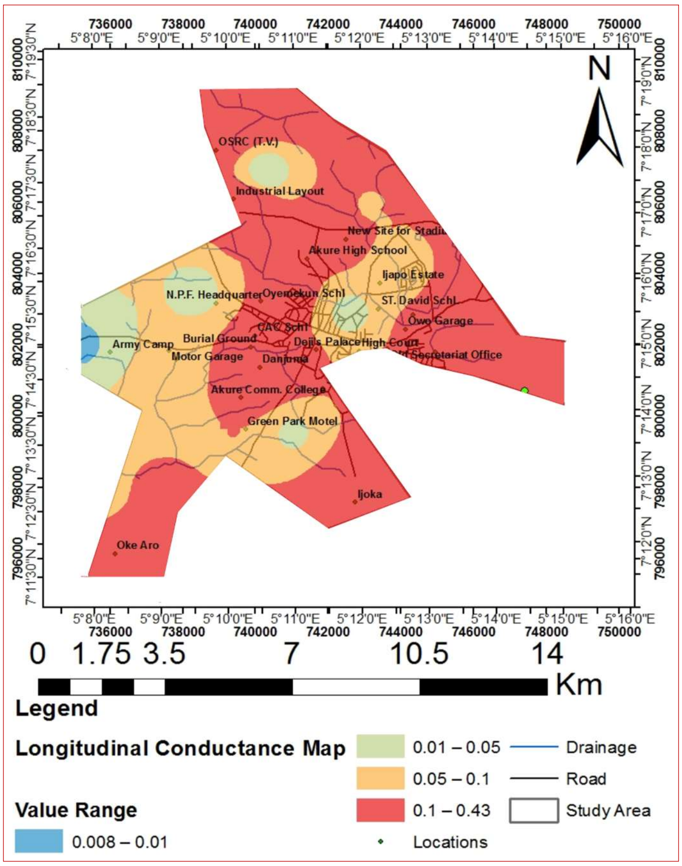


Fig. 13. Longitudinal conductance map of the study area

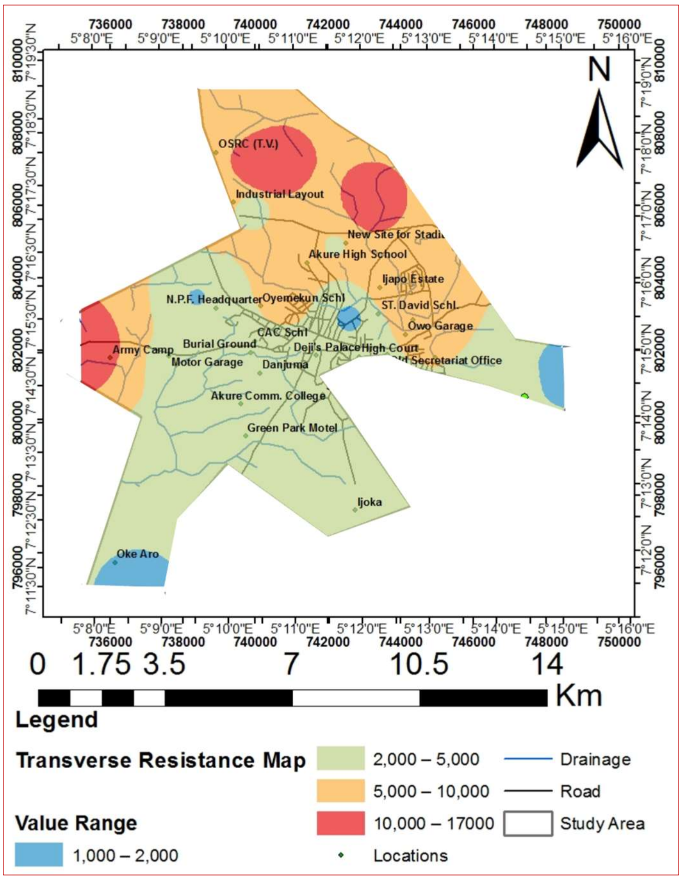


Fig. 14. Transverse resistance map of the study area

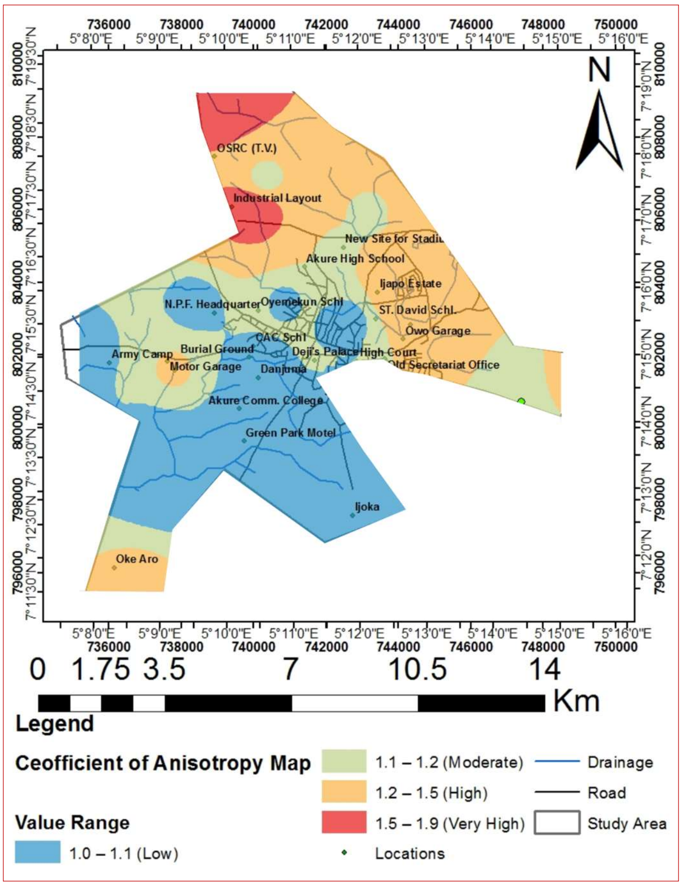


Fig. 15. Coefficient of anisotropy map of the study area

The map was categories into four groundwater prospect region which were low, moderate, high and very high while area with high and very high values of coefficient of anisotropy suggests that the fracture system must have extended in all the directions with different degrees of fracturing, which had greater water holding capacity from different directions of the fracture(s) within the rock resulting in higher porosity.

### 4.6. Modeling of groundwater potential

The groundwater potential rate (R) gives the ranges of groundwater storage potentiality within each parameter. Each parameter was classified and rated. However, since resistivity and thickness do not have the same units, a unified scaling technique was adopted in rating these parameters according to their degree of influence on groundwater occurrence (Adiat et al., 2013; Ilugbo et al., 2018b). Therefore, different range of values or features should have a different rating (R) in a scale according to its importance in accumulating groundwater. In this study, each parameter has been scored in the 1–5 scale in the ascending order of hydrogeologic significance. However, the resistivity range of any given rock type is wide and overlaps with other rock types. Coefficient of anisotropy, overburden thickness, aquifer resistivity, aquifer thickness and geology in the area were considered to obtain the classifications and ratings shown in Table 1. The groundwater potential index obtained for each location was interpolated, using inverse distance weighting (IDW) techniques in ArcGIS 10.5 to produce the groundwater potential map shown in Fig. 16 and the zones are summarized in Table 2. The groundwater potential map further assisted in better understanding as well as evaluating the groundwater prospect of the study area with small closure at the northern and eastern parts has the highest prospect for groundwater. Majority of the area was characterized as moderate to high groundwater prospect with small closure at western and northeastern part has a low groundwater prospect.

Table 1. Probability rating (R) for classes of the parameters

| Influencing factors | Category (Classes) | Potential of groundwater storage | Rating (R) | Normalized weight (W) |
|---|---|---|---|---|
| Coefficient of anisotropy | 1.0 – 1.1 | Low | 2 | 0.41 |
| | 1.1 – 1.2 | Moderate | 3 | |
| | 1.2 – 1.9 | High | 4 | |
| | | Very High | 5 | |
| Aquifer resistivity | 0 – 100 | Low | 2 | 0.27 |
| | 100 – 150 | Moderate | 3 | |
| | 150 – 250 | High | 4 | |
| | 250 - 374 | Moderately low | 3 | |
| Overburden thickness | 6.7 – 10 | Very Low | 1 | 0.16 |
| | 10 – 15 | Low | 2 | |
| | 15 – 20 | Moderate | 3 | |
| | 20 – 39.9 | High | 4 | |
| Aquifer thickness | 0 – 5 | Very Low | 1 | 0.11 |
| | 5 – 10 | Low | 2 | |
| | 10 – 15 | Moderate | 3 | |
| | 15 – 36.5 | High | 4 | |
| Geology | Biotite Gneiss | - | 2 | 0.05 |
| | Charnockite | | 2 | |
| | Granite Gneiss | | 2 | |
| | Migmatite Gneiss | | 3 | |
| | Polfic Schist | | 2 | |
| | Porhyritic Granite | | 3 | |
| | Quartzite | | 3 | |

Table 2: Groundwater potential classifications

| Groundwater potential values | Classifications |
|---|---|
| 0.69 – 1.5 | Low |
| 1.5 – 2.5 | Moderate |
| 2.5 – 3.0 | High |
| 3.0 – 3.94 | Very High |

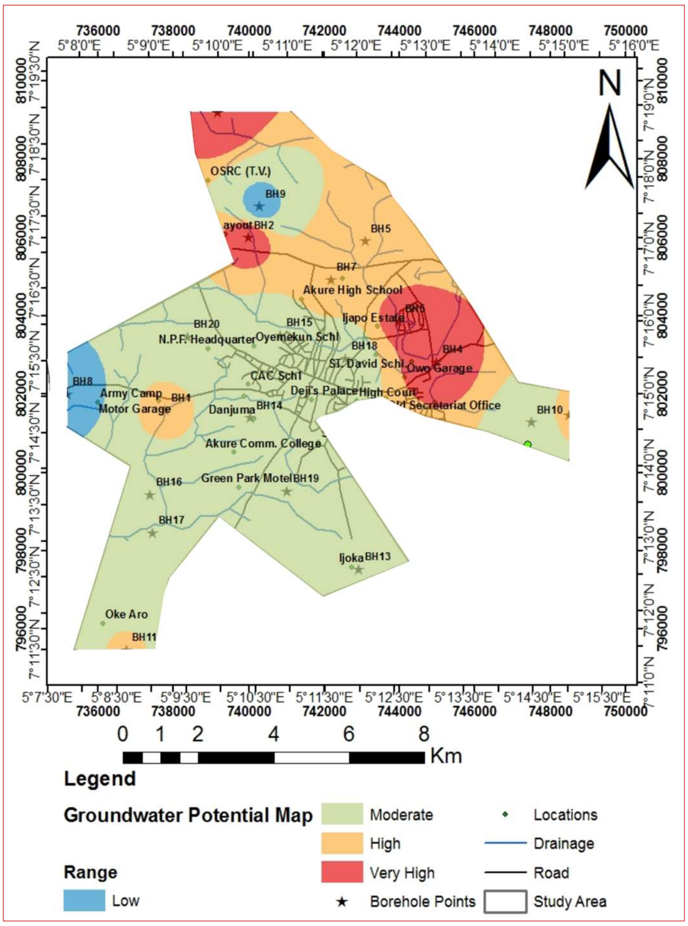


Fig. 16. Groundwater potential map of the study area

## 4.7. Groundwater yield map

M-formula was used to determine the groundwater yield index which was used to model groundwater yield map of the study area which has been able to combine all variable factors associated with groundwater prospect (Fig. 17). The small closure at the Eastern, Northwestern and Southeastern parts has very high and high groundwater yield while most of the remaining area has moderate yield expect a small closure at the Eastern and Southwestern parts has low groundwater yield.

## 5. Conclusion

The study has revealed the usefulness of apparent resistivity contrast as a viable tool for structural mapping to compensate for magnetic, electromagnetic, gravity and seismic refraction for groundwater exploration. Due to the complex geology of a Typical Crystalline Basement Complex, as in the case of Southwestern Nigeria, random VES is not enough in search for viable groundwater resource of this region. It is strongly recommended that for any groundwater exploration activities, in absence of magnetic, electromagnetic, gravity and seismic refraction, the use of LRP or 2D resistivity imaging for structural evaluation becomes a matter of high necessity and inevitable scientific approach before carryout VES.

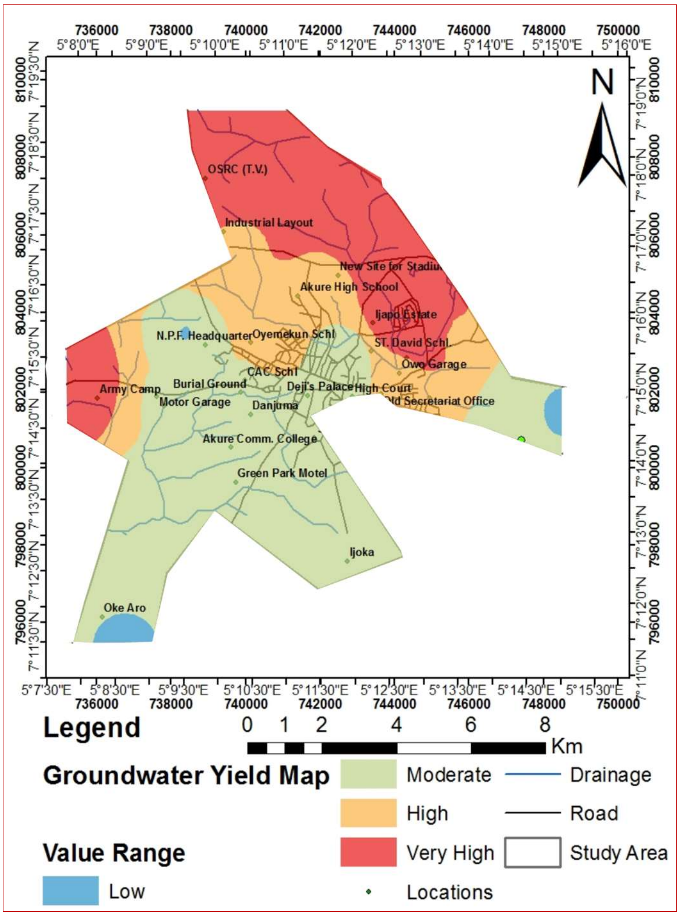


Fig. 17. Groundwater yield of the study area

## Acknowledgement

The authors gratefully acknowledge Prof. Aina A.O., Prof. Ojo J.S. and Prof. Olorunfemi M.O. for their valuable contribution at improving the quality of this research work.

## References

Adebiyi, A.D., Ilugbo, S.O., Bamidele, O.E., Egunjobi, T., 2018. Assessment of Aquifer Vulnerability Using Multi- Criteria Decision Analysis around Akure Industrial Estate, Akure, Southwestern Nigeria. Journal of Engineering Research and Reports 3 (3), 1-13.

Adebo, B.A., Layade, G.O., Ilugbo, S.O., Hamzat, A.A., Otobrise, H.K., 2019. Mapping ofSubsurface Geological Structures using Ground Magnetic and Electrical Resistivity Methods within Lead City University, Southwestern Nigeria. Kada Journal of Physics 2 (2), 64-73.

Adebo, A.B., Ilugbo, S.O., Oladetan, F.E., 2018. Modeling of Groundwater Potential Using Vertical Electrical Sounding (VES) and Multi-caterial Analysis at Omitogun Housing Estate, Akure, Southwestern Nigeria. Asian Journal of Advanced Research and Reports 1 (2), 1-11.

Adiat, K.A.N., Nawawi, M.N.M., Abdullah, K., 2013. Application of Multi-Criteria Decision Analysis to Geoelectric and Geology Parameters for Spatial Prediction of Groundwater Resources Potential and Aquifer Evaluation. Pure Applied Geophysics 170 (3), 453–471.

Alabi, T.O., Ilugbo, S.O., Akinmoye, O.E., Ibitomi, M.A., Aigbedion, I., Adeleke, K.A., Ajanaku, B.S., 2019. Application of Electrical Resistivity and Hydrochemistry Methods for Mapping Groundwater Contamination around Okun Ilashe Island Area, Lagos State, Southwestern Nigeria, Journal of Geography, Environment and Earth Science International 23 (4), 1-15.

Aluko, A.B., 2008. Geology of Akure Area Southwestern Nigeria. Unpublished B.Tech. Thesis, Federal University of Technology, Akure, 70.

Bawallah, M.A., Ofomola, M.O., Ilugbo, S.O. Aina, A.O., Olaogun, S.O., Olayiwola, K.O, Awoniran D.R., 2020. Effect of Lineament and drainage orientation on groundwater potential of Moro Area Central Kwara State Nigeria. Indian Journal of Science and Technology 13 (10), 1124-1134.

Bawallah, M.A., Aina, A.O., Ilugbo, S.O., Ozegin, K.O., Olasunkanmi, K.N., 2018). Evaluation of Groundwater Yield Capacity Using Dar-zarrouk Parameter of Central Kwara State, Southwestern Nigeria. Asian Journal of Geological Research 1 (1), 1-13.

Chowdhury, A., Jha, M.K., Chowdary, V.M., Mal, B.C., 2009. Integrated remote sensing and GIS based approach for assessing groundwater. International Journal of Remote Sensing 30 (1), 231-250.

Eastman, J.R., 1996. Multi-criteria Evaluation and Geographical Information Systems Eds. Longley PA, Goodchild MF, Magurie DJ and Rhind DW, Second Edition, 1 (John Wiley and Sons, New York), 493-502.

Ewusi, A., Kuma, J.S., Voigt, H.J., 2009. Utility of the 2-D multi-electrode resistivity imaging technique in groundwater exploration in the Voltaian sedimentary basin, Northern Ghana. Natural Resources Research 18 (4), 267-275.

Ilugbo, S.O., Adebo, B.A., Olomo, K.O., Adebiyi, A.D., 2018a. Application of Gis and multi criteria decision analysis to geoelectric parameters for modeling of groundwater potential around Ilesha, Southwestern Nigeria. European Journal of Academic Essays 5 (5), 105-123.

Ilugbo, S.O., Adebiyi, A.D., Olomo, K.O., 2018b. Modeling of Groundwater Yield Using GIS and Electrical Resistivity Method in a Basement Complex Terrain, Southwestern Nigeria, Journal of Geography, Environment and Earth Science International 16 (1), 1-17.

Ilugbo, S.O., Edunjobi, H.O., Alabi, T.O., Ogabi, A.F., Olomo, K.O., Ojo, O.A., Adeleke, K.A., 2019. Evaluation of Groundwater Level Using Combined Electrical Resistivity Log with Gamma (Elgg) around Ikeja, Lagos State, Southwestern Nigeria. Asian Journal of Geological Research 2 (3), 1-13.

Ilugbo, S.O., Adebiyi, A.D., 2017. Intersection of lineaments for groundwater prospect analysis using satellite remotely sensed and aeromagnetic dataset around Ibodi, Southwestern Nigeria. International Journal of Physical Sciences 12 (23), 329-353.

Lee, S., Song, K-Y., Kim, Y., Park, I., 2012. Regional groundwater productivity potential mapping using a geographic information system (GIS) based artificial neural network model. Hydro-geology Journal 20, 1511-1527.

Murali, S., Patangay, N.S., 1998. Principles and applications of groundwater Geophysics, Publ. by AEG, OU, Hyderabad: Association of Exploration Geophysicists p. 421.

Navalgund, R.R., 1997. Revised development plan of Ahmedabad Urban Development Authority Area-2011. Ahmedabad Urban Development Authority and Space Applications Centre, Ahmedabad, India, Technical Report 1 SAC/RSAG/TR/12/ AUG/1997, 142.

Odeyemi, I.B., Asiwaju-Bello, Y.A., 1999. Anifowose AYB. Remote sensing fracturecharacteristics of the pan African granite batholiths in the basement complex of parts of Southwestern Nigeria. Journal of Techno-Science 3, 56-60.

Olarewaju, V.O., 1988. REE in charnockitic and associated granitic rocks of Ado-Ekiti Akure, Southwest Nigeria: In: Precambrian Geology of Nigeria. (Edited by the Nigerian Geological Survey), 231-239.

Olorunfemi, M.O., Olarewaju, V.O., Alade, O., 1991. On the electrical anisotropy and Ground water yield in a Basement complex area of S.W. Nigeria. Journal of African Earth Sciences (and the Middle East) 12 (3), 462-472.

Owoyemi, F.B., 1996. A geologic-geophysical investigation of rain-induced erosional features in Akure Metropolis. Unpublished M.Sc. Thesis, Federal University of Technology, Akure, 11-18.

Oyedele, AA., Bawallah, M.A., Ozegin, K.O., Ilugbo, S.O., Ajayi, C.A., Aigbedion, I., 2020. Probability functions of road failures in a typical basement complex region, South western Nigeria: A case study of Akure - Oba Ile Airport Road. International Journal of Water Resources and Environmental Engineering 12 (2), 10-21.

Oyedele A.A., 2019. Use of remote sensing and GIS techniques for groundwater exploration in the basement complex terrain of Ado-Ekiti, SW Nigeria. Applied Water Science 9, 51.

Ozegin, K.O., Bawallah, M.A., Ilugbo, S.O., Oyedele, A.A., Oladeji, J.F., 2019. Effect of Geodynamic Activities on an Existing Dam: A Case Study of Ojirami Dam, Southern Nigeria. Journal of Geoscience and Environment Protection 7, 200-213.

Rahaman, M.A., 1988. Recent advances in the study of the basement complex of Nigeria. In Oluyide PO, Mbonu WC, Ogezi AE, Egbuniwe IG, Ajibade AC, Umeji AC. (Eds.). Precambrian Geology of Nigeria. Geological Survey of Nigeria Special Publication 11, 41.

Slomczynska, B., Slomczynski, T., 2004. Physicochemical and toxicological characteristics of Leachates from MSW Landfills. Polish Journal of Environmental Studies 13 (6), 627-637.

Singhal, D.S., Niwas, S., 1981. Examination of aquifer transmissivity from Dar Zarrouk parameters in porous media, Journal of Hydrology 50, 393-399.